(12) (19) (CA) **Demande-Application**

O P I C
OFFICE DE LA PROPRIÉTÉ INTELLECTUELLE DU CANADA

C I P O
CANADIAN INTELLECTUAL PROPERTY OFFICE

(21) (A1) **2,292,357**
(22) 1999/12/17
(43) 2000/06/18

(72) STINSON, MICHAEL R., CA
(72) RYAN, JAMES G., CA
(71) NATIONAL RESEARCH COUNCIL OF CANADA, CA
(51) Int.Cl.[7] H04R 1/40
(30) 1998/12/18 (60/112,950) US
(54) **STRUCTURE DE DIFFRACTION DE RESEAU DE MICROPHONES**
(54) **MICROPHONE ARRAY DIFFRACTING STRUCTURE**

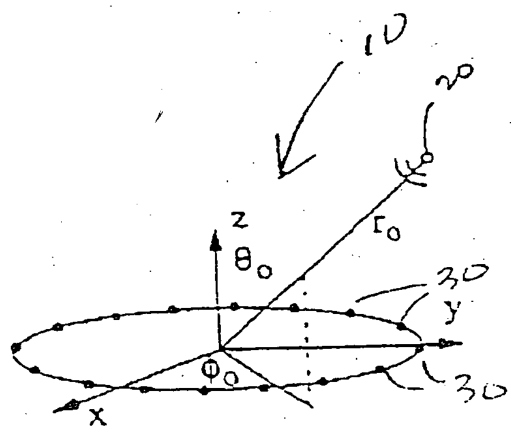

(57) The present invention increases the aperture size of a microphone array by introducing a diffracting structure into the interior of a microphone array. The diffracting structure within the array modifies both the amplitude and phase of the acoustic signal reaching the microphones. The diffracting structure increases acoustic shadowing along with the signal's travel time around the structure. The diffracting structure in the array effectively increases the aperture size of the array and thereby increases the directivity of the array. Constructing the surface of the diffracting structure such that surface waves can form over the surface further increases the travel time and modifies the amplitude of the acoustical signal thereby allowing a larger effective aperture for the array.

MICROPHONE ARRAY DIFFRACTING STRUCTURE

Field of the Invention

The present invention relates to microphone technology and specifically to microphone arrays which can achieve enhanced acoustic directionality by a combination of both physical and signal processing means.

Background of the Invention

Microphone arrays are well known in the field of acoustics. By combining the outputs of several microphones in an array electronically, a directional sound pickup pattern can be achieved. This means that sound arriving from a small range of directions is emphasized while sound coming from other directions is attenuated. Such a capability is useful in areas such as telephony, teleconferencing, video conferencing, hearing aids, and the detection of sound sources outdoors. However, practical considerations mitigate against physically large arrays. It is therefore desirable to obtain as much acoustical directionality out of as small an array as possible.

Normally, reduced array size can be achieved by utilizing superdirective approaches in the combining of microphone signals rather than the more conventional delay and sum beamforming usually used in array signal processing. While superdirective approaches do work, the resulting array designs can be very sensitive to the effects of microphone self noise and errors in matching microphone amplitude and phase responses.

microphone arrays. Elko et al however, utilizes costly signal processing means to reduce noise. The signal processing capabilities required to keep adaptively calculating the required real-time analysis can be prohibitive.

A further patent, issued to Gorike, U.S. Patent 4,904,078 uses directional microphones in eyeglasses to assist persons with a hearing disability receiving aural signals. The directional microphones, however, do not allow for a changing directionality as to the source of the sound.

The use of diffraction can effectively increase the aperture size and the directionality of a microphone array. Thus, diffractive effects and the proper design of diffractive surfaces can provide large aperture sizes and improved directivity with relatively small arrays. When implemented using superdirective beamforming, the resulting array is less sensitive to microphone self noise and errors in matching microphone amplitude and phase responses. A simple example of how a diffracting object can improve the directional performance of a system is provided by the human head and ears. The typical separation between the ears of a human is 15 cm. Measurements of two-ear correlation functions in reverberant rooms show that the effective separation is more than double this, about 30 cm, which is the ear separation around a half-circumference of the head.

Academic papers have recently suggested that diffracting structures can be used with microphone arrays. An oral paper by Kawahara and Fukudome, ("Superdirectivity design for a sphere-baffled microphone", J. Acoust. Soc. Am. 130,2897, 1998),

directivity of the array. Constructing the surface of the diffracting structure such that surface waves can form over the surface further increases the travel time and modifies the amplitude of the acoustical signal thereby allowing a larger effective aperture for the array.

In one embodiment, the present invention provides a diffracting structure for use with a microphone array, the microphone array being comprised of a plurality of microphones defining a space generally enclosed by the array wherein a placement of the structure is chosen from the group comprising the structure is positioned substantially adjacent to the space; and at least a portion of the structure is substantially within the space; and wherein the structure has an outside surface.

In another embodiment, the present invention provides a microphone array comprising a plurality of microphones constructed and arranged to generally enclose a space; a diffracting structure placed such that at least a portion of the structure is adjacent to the space wherein the diffracting structure has an outside surface.

A further embodiment of the invention provides a method of increasing an apparent aperture size of a microphone array, the method comprising; positioning a diffraction structure within a space defined by the microphone array to extend a travel time of sound signals to be received by microphones in the microphone array, generating different time delay weights, phases, and amplitudes for signals from each microphone in the microphone array, applying said time delay weights to said sound signals received by each microphone in the

Figures 7A to 24A illustrates top views of some possible diffracting structures and microphone arrays.

Figures 7B to 24B illustrate corresponding side view of the diffracting structures of Figures 7A to 24A.

Figure 25 is a plot comparing the directivity of a circular array having a diffracting structure within the array with the directivity of the same circular array without the diffracting structure.

Figure 26 illustrates the construction of a surface wave propagating surface for the diffracting structures.

Figure 27 plots the surface wave phase speed for a simple celled construction as pictured in Fig 17; and

Figures 28-31 illustrate different configurations for coating the diffracting surface.

Figure 32 is a plot of the directional beam response for a hemispherical diffracting structure. The plots for a rigid and a soft diffracting structure are plotted on the same graph for ease of comparison.

Figure 33 is the diffracting structure used for Figure 32.

Figure 34 is a cross-sectional diagram of the cellular structure of the diffracting structure shown in Fig 33.

Figure 35 is a preferred embodiment of a microphone array utilizing the methods and concepts of the invention.

Figure 36 is a plot of the beamformer response obtained using the microphone array of Figure 35 both with and without a cellular structure and with optimization.

time delay τ_m so that all microphone contirbutions are in phase when sound comes form a desired direction. This approach is equivalent to delay-and-sum beamforming for an array in free space. When acoustical noise is present, improved beamforming performance can be obtained by applying optimization techniques, as discussed below.

The acoustic pressure signal p_m from microphone m consists of both a signal component s_m and a noise component n_m where

$$p_m = s_m + n_m$$

An array is designed to enhance reception of the signal component while suppressing reception of the noise component. The array's ability to perform this task is described by a performance index known as array gain.

Array gain is defined as the ratio of the array output signal-to-noise ratio over that of an individual sensor. For a specific frequency ω the array gain $G(\omega)$ can be written using matrix notation as

$$G(f) = \frac{E\{|W^H S|^2\} / (E\{|W^H N|^2\})}{\sigma_s^2 / \sigma_n^2} = \frac{E\{W^H S \cdot S^{HW\}/} \sigma_s^2}{E\{W^H N \cdot N^H W\} / \sigma_n^2} \tag{1}$$

In this expression, W is the vector of sensor weights

$$G(\omega)=\frac{W^H R_{ss}(\omega)W}{W^H R_{nn}(\omega)W}. \qquad (4)$$

The array gain is thus described as the ratio of two quadratic forms (also known as a Rayleigh quotient). It is well known in the art that such ratios can be maximized by proper selection of the weight vector W. Such maximization is advantageous in microphone array sound pickup since it can provide for enhanced array performance for a given number and spacing of microphones simply by selecting the sensor weights W.

Provided that $R_{nn}(\omega)$ is non-singular, the value of $G(\omega)$ is bounded by the minimum and maximum eigenvalues of the symmetric matrix $R_{nn}^{-1}(\omega)R_{ss}(\omega)$. The array gain is maximized by setting the weight vector W equal to the eigenvector corresponding to the maximum eigenvalue.

In the special case where $R_{ss}(\omega)$ is a dyad, that is, it is defined by the outer product

$$R_{ss}(\omega)=SS^H \qquad (5)$$

then the weight vector W_{opt} that maximizes $G(\omega)$ is given simply by

$$W_{opt}=R_{nn}^{-1}(\omega)S. \qquad (6)$$

It has been shown that the optimum weight solutions for several different optimization strategies

Regarding gain maximization with a white-noise gain constraint, white noise gain is defined as the array gain against noise that is incoherent between sensors. The noise correlation matrix in this case reduces to an *M x M* identity matrix. Substituting this into the expression for array gain yields

$$G_w(\omega) = \frac{W^H R_{ss}(\omega) W}{W^H I W} \qquad (8)$$

White noise gain quantifies the array's reduction of sensor and preamplifier noise. The higher the value of $G_w(\omega)$, the more robust the beamformer. As an example, the white noise gain for an *M*-element delay-and-sum beamformer steered for plane waves is *M*. In this case, array processing reduces uncorrelated noise by a factor of *M* (improves the signal-to-noise ratio by a factor of *M*).

A white noise gain constraint is imposed on the gain maximization procedure by adding a diagonal component to the noise correlation matrix. That is, replace $R_{nn}(\omega)$ by $R_{nn}(\omega)+\kappa I$. The strength of the constraint is controlled by the magnitude of κ. Setting κ to a large value implies that the dominant noise is uncorrelated from microphone to microphone. When uncorrelated noise is dominant, the optimum weights are those of a conventional delay-and-sum beamformer. Setting $\kappa = 0$, of course, produces the unconstrained optimum array. Unfortunately, there is no simple relationship between the constraint parameter κ and the

than that observed in the acoustic shadow zone. This means that the relative importance of microphone noise varies substantially with the different microphone positions. Similarly, the effects of microphone gain and phase tolerances also vary widely with microphone location.

To obtain a practical design in the presence of amplitude and phase variations, an expression for the expected array gain must be obtained. The analysis of this problem is facilitated by assuming that the actual array weights described by the vector $\boldsymbol{W}$ vary in amplitude and phase about their nominal values $\boldsymbol{W_0}$. Assuming zero-mean, normally distributed fluctuations it is possible to evaluate the expected gain of the beamformer. The expression is

$$E\{G(\omega)\} = \frac{e^{-\sigma_p^2}(W_0{}^H R_{ss}(\omega) W_0) + \left(1 - e^{-\sigma_p^2} + \sigma_m^2\right)(W_0{}^H diag(R_{ss}(\omega)) W_0)}{e^{-\sigma_p^2}(W_0{}^H R_{nn}(\omega) W_0) + \left(1 - e^{-\sigma_p^2} + \sigma_m^2\right)(W_0{}^H diag(R_{nn}(\omega)) W_0)} \qquad (9)$$

where σ_m^2 is the variance of the magnitude fluctuations and σ_p^2 is the variance of the phase fluctuations due to microphone tolerance.

Although this expression is more complicated than that shown in (4), it is still a ratio of two quadratic forms. Provided that the matrix $\boldsymbol{A}$ is non-singular, the value of the ratio is bounded by the minimum and maximum eigenvalues of the symmetric matrix

$$A^{-1}B$$

where

θ_o = angle to the positive z-axis as shown in Figure 1

ϕ_o = angle to the positive x-axis as shown in Figure 1)

the pressures at each microphone 30 is given by Equation 11:

$$p_{mo} = \frac{C\exp(ikr_{mo})}{kr_{mo}}, \qquad (11)$$

where C is a source strength parameter and the distances between source and microphones are

$$r_{mo} = [r_o^2 + a^2 - 2r_o a \sin\theta_o \cos(\phi_m - \phi_o)]^{1/2};$$

where a is the radius of the circle, ϕ_m is the azimuthal position of microphone m. The array output is thus given by Equation 12:

$$V \propto \sum_{m=1}^{m} p_{mo} e^{(+i\omega\tau_m)} \qquad (12)$$

Suppose it is desired to steer a beam to a look position (r_l, θ_l, ϕ_l), where θ_l is the azimuth and ϕ_l is the elevation angle. The pressure p_m that would be obtained at each microphone position if the source was at this look position are

The response function in Figure 3 can be improved upon by inserting a diffracting structure inside the array. An example of this is pictured in Figure 4.

Figure 4 illustrates a circular array with a spherical diffracting structure positioned within the array.

Figure 5 illustrates another configuration using a diffracting structure. Figure 5 shows a bi-circular array 50 with a diffracting structure 60 mostly contained within the space defined by the bi-circular array 50.

To determine the response function for an array such as that pictured in Figure 4, some of the assumptions made in calculating the response function shown in Figure 3 cannot be made. While the above equations assume that the pressure at each microphone was the free-field sound pressure due to a point source, such is not the case with an array having a diffracting structure. A diffracting structure should have a surface S that can be defined by an acoustic impedance function. Subject to the appropriate boundary conditions on the surface S of the diffracting structure 60, the acoustic wave equation will have to be solved to determine the sound pressure over the surface. Diffraction and scattering effects can then be included in the beamforming analysis.

For such an analysis, a source at a position given by $r_o=(r_o, \theta_o, \phi_o)$ is assumed. For this source, the boundary value problem is given by Equation 14:

$$\nabla^2 p + k^2 p = \delta(r - r_o) \qquad (14)$$

Evaluating the pressure p_{mo} at each microphone position r_m we have:

$$p_{mo} = F(r_m, r_o)$$

giving a uniform weight beamformer output (Equation 17)

$$V \propto \sum_{m=1}^{M} F(r_m, r_o)\exp(i\omega\tau_m). \qquad (17)$$

The pressure at each microphone will vary significantly in both magnitude and phase because of diffraction.

Suppose that a beam is to be steered toward a look position $r_l=(r_l, \theta_l, \phi_l)$. The microphone pressures that would be obtained if this look position corresponded to the actual source position would be

$$p_{ml} = F(r_m, r_l)$$

The time delays τ_m are then set according to Equation 18

$$\omega\tau_m = -\arg[F(r_m, r_l)] \qquad (18)$$

where $\arg[Fr_m, r_l)]$ denotes the argument of the function $F(r_m, r_l)$.

As noted above, Figure 4 shows an example of the above. Figure 4 is a circular array 70 on the

650Hz point source was located in the plane of the microphones with $r_0=2$, $\theta_0=\pi/2$, and $\phi_0=0$. The look position has $r_l = 2m$ and $\theta_l = \pi/2$ fixed. The response V as a function of azimuthal look angle ϕ_l is shown as the solid line in Figure 6. For comparison, the beamformer response obtained with no sphere has been calculated using Equation 13 and this result shown as the dashed line in Figure 6.

The inclusion of the diffracting sphere is seen to enhance the performance of the array by reducing the width of the central beam.

While the circular array was convenient for its mathematical tractability, many other shapes are possible for both the microphone array and the diffracting structure. Figures 7 to 24 illustrate these possible configurations.

The configurations pictured with a top view and a side view are as follows:

	Microphone Array	Diffracting Structure
Figures 7A & B	Circular	hemisphere
Figures 8A & B	bi-circular	hemisphere
Figures 9A & B	circular	right circular cylinder
Figures 10A & B	circular	raised right circular cylinder
Figures 11A & B	circular	cylinder with a star shaped cross section
Figures 12A & B	square pyramid	truncated square pyramid

Figure 21A & B	square	circular shape with a convex top and a flared square base opening to the circular shape
Figure 22A & B	square	truncated square pyramid
Figure 23A & B	hexagonal	truncated hexagonal pyramid
Figure 24A & B	hexagonal	shallow hexagonal solid cylinder raised from the surface by a hexagonal stand

It should be noted that in the above described figures, the black dots denote the position of microphones in the array. Other shapes not listed above are also possible for the diffracting structure.

As can be seen from Figures 7 to 24, the placement of the microphone array can be anywhere as long as the diffracting structure, or at least a portion of it, is contained within the space defined by the array.

To determine the improvement in spatial response due to a diffracting structure, the directivity index D is used. This index is the ratio of the array response in the signal direction to the array response averaged over all directions. This index is given by equation 20:

be reduced in size by a factor of 1.4 and have approximately the same performance as the array with no sphere. This 30% reduction in size would be very important to designers of products such as handsfree telephones or arrays for hearing aids where a smaller size is important. Moreover, once the size is reduced, the number of microphones could be reduced as well.

Additional performance enhancements can be obtained by appropriate treatment of the surface of the diffracting objects. The surfaces need not be acoustically-rigid as assumed in the above analysis. There can be advantages in designing the exterior surfaces to have an effective acoustical surface impedance. Introducing some surface damping (especially frequency dependent damping) could be useful in shaping the frequency response of the beamformer. There are however, particular advantages in designing the surface impedance so that the air-coupled surface waves can propagate over the surface. These waves travel at a phase speed lower than the free-field sound speed. Acoustic signals propagating around a diffracting object via these waves will have an increased travel time and thus lead to a larger effective aperture of an array.

The existence and properties of air-coupled surface waves are known in the art. A prototypical structure with a plurality of adjacent cells is shown in Figure 26. A sound wave propagating horizontally above this surface interacts with the air within the cells and has its propagation affected. This may be understood in terms of the effective acoustic surface impedance Z of the structure. Plane-wave-like solutions of the Helmholtz equation,

propagation within the cells may be assumed to be one dimensional. For the simple cells of depth L shown in Figure 17, the effective surface impedance is

$$Z = i\rho c \cot kL,$$

so surface waves are possible for frequencies less than the quarter-wave resonance.

To exploit the surface-wave effect, microphones may be mounted anywhere along the length of the cells. At frequencies near cell resonance, however, the acoustic pressure observed at the cell openings and at other pressure nodal points will be very small. To use the microphone signals at these frequencies, the microphones should be located along the cell's length at points away from pressure nodal points. This can be achieved for all frequencies if the microphones are located at the bottom of the cells since an acoustically rigid termination is always an antinodal point.

The phase speed of a propagating surface wave is

$$c_{ph} = \omega / \mathrm{Re}\{\ \alpha\}$$

For the simple surface structure shown in Figure 26, using a cell depth of L=2.5 cm, we obtain the phase speed shown in Figure 27. The phase speed is the free-field sound speed at low frequencies but drops gradually to zero at about 3400 Hz. Above this frequency, the reactance is negative and no surface wave can propagate. The reduced phase speed increases the travel time for

surface impedance, at the hemisphere surface, that is spring-like at 650 Hz. For the response patterns shown in Figure 32, a 650 Hz point source was located in the plane of the microphones 110 with $r_0 = 2$, $\theta_l = \pi/2$, and $\phi_0 = 0$. The look position has r_l = 2m and $\theta_l = \pi/2$ fixed. The response V as a function of azimuthal look angle ϕ_l is shown as the solid line in Figure 32. The dashed line shows the response obtained for a rigid hemisphere with te microophones located on the outer surface at the base of the hemisphere.

The inclusion of the surface treatment is seen to enhance the array performance substantially. The width of the main beam at half height is reduced from ± 147° for the rigid sphere to ±90° for the soft sphere. Furthermore, the directivity index at 650 Hz increases by 2.4dB.

The cellular surface described is one method for obtaining a desired acoustical impedance. This approach is attractive since it is completely passive and the impedance can be controlled by modifying the cell characteristics but there are practical limitations to the impedance that can be achieved.

Another method to provide a controlled acoustical impedance is the use of active sound control techniques. By using a combination of acoustic actuator (e.g. loudspeaker), acoustic sensor (e.g. microphone) and the appropriate control circuitry a wider variety of impedance functions can be implemented. (See for example US Patent number 5812686).

A design which encompasses the concepts disclosed above is depicted in Fig. 35. The design in Fig 35 is of a diffracting structure with a convex top 130 and an

technique. Directivity indices achieved using delay-and-sum and optimized beamforming are shown in Figure 36 as a function of frequency. Results are shown for the housing with no cells (dashed line) as well as for the housing with three rows of cells open as described above (solid line). Also shown are results for the housing with cells and optimization (dash and dot lines). As seen in Figure 36, the use of cells to control the surface impedance has a beneficial effect on the directivity index. An increase in directivity index is observed between 550 Hz to 1.6kHz with a boost of approximately 4 dB obtained in the range of 700Hz to 800Hz. The use of array-gain optimization, as described by equation 9, is shown in Figure 36 to further increase the directivity of the device by approximately 6 dB at 200 Hz.

The person understanding the above described invention may now conceive of alternative design, using the principles described herein. All such designs which fall within the scope of the claims appended hereto are considered to be part of the present invention.

5. A structure as claimed in claim 2 wherein the first set of portions has a cell-like construction.

6. A structure as claimed in claim 4 wherein the outside surface of the structure has a cell-like construction.

7. A structure as claimed in claim 1 wherein the structure has a shape chosen from the group comprising:

a) hemisphere
b) right circular cylinder
c) a cylinder with a star shaped cross section
d) a square truncated pyramid
e) an inverted truncated pyramid with a generally square cross section
f) a right circular cylinder coupled to a flattened oblate spheroid at each end of the cylinder
g) an oblate spheroid
h) a flat shallow solid cylinder
i) a shallow solid cylinder with a convex top
j) generally circular with a convex top
k) shallow cup shaped cross section
l) shallow solid cylinder
m) generally circular with a convex top
n) hexagonal truncated pyramid and
o) shallow hexagonal solid cylinder

8. A structure as claimed in claim 7 wherein the outside surface of the structure has a cell-like construction.

coupled surface waves to propagate over a first set of portions.

14. An array as claimed in claim 13 wherein a second set of portions of the outside surface of the structure is constructed and arranged to absorb and dampen sound.

15. An array as claimed in claim 11 wherein the outside surface of the structure is constructed and arranged to allow air-coupled surface waves to propagate over the outside surface.

16. An array as claimed in claim 13 wherein the first set of portions has a cell-like construction.

17. An array as claimed in claim 15 wherein the outside surface of the structure has a cell-like construction.

18. An array as claimed in claim 11 wherein a shape of the structure is chosen from the group comprising:

a) hemisphere
b) right circular cylinder
c) a cylinder with a star shaped cross section
d) a square truncated pyramid
e) an inverted truncated pyramid with a generally square cross section
f) a right circular cylinder coupled to a flattened oblate spheroid at each end of the cylinder
g) an oblate spheroid and
h) a flat shallow solid cylinder

21. An array as claimed in claim 20 wherein the outside surface of the structure has a cell-like construction and wherein the microphones are disposed within the cells.

22. A method of increasing an apparent aperture size of a microphone array, the method comprising:

a) positioning a diffraction structure within a space defined by the microphone array to extend a travel time of sound signals to be received by microphones in the microphone array;

b) generating different time delay weights, phases, and amplitudes for signals from each microphone in the microphone array;

c) applying said time delay weights to said sound signals received by each microphone in the microphone array

wherein

the diffraction structure has a shape;

said time delay weights are determined by analyzing the shape of the diffraction structure and the travel time of the sound signals.

23. A method as claimed in claim 16 wherein the shape of the structure is chosen from the group comprising:

a) hemisphere

b) right circular cylinder

c) a cylinder with a star shaped cross section

d) a truncated square pyramid

e) an upside down truncated square pyramid

28. A method as claimed in claim 26 further including constructing and arranging the outside surface of the diffraction structure to have a cell-like construction.

29. A microphone array for use on a generally flat surface comprising:

a body having a convex top and an inverted truncated cone for a bottom;

a plurality of cells located on a surface of the bottom for producing an acoustic impedance; and

a plurality of microphones located adjacent to the bottom.

30. A microphone array as claimed in claim 29 wherein each of the plurality of microphones is placed inside a cell chosen from the plurality of cells.

31. A microphone array as claimed in claim 29 further including a speaker located substantially in a center of the convex top.

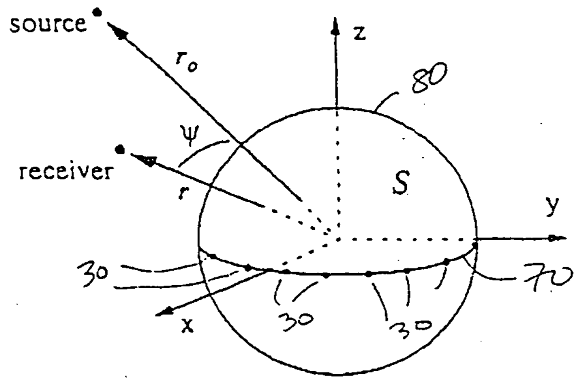

FIG 4

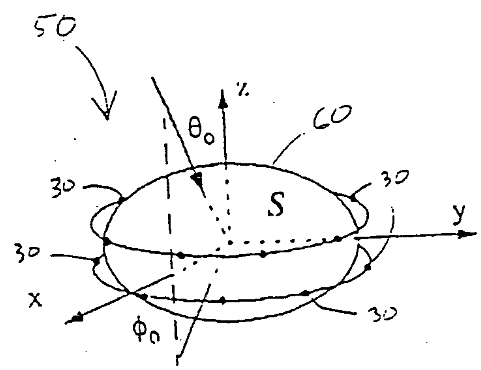

FIG 5

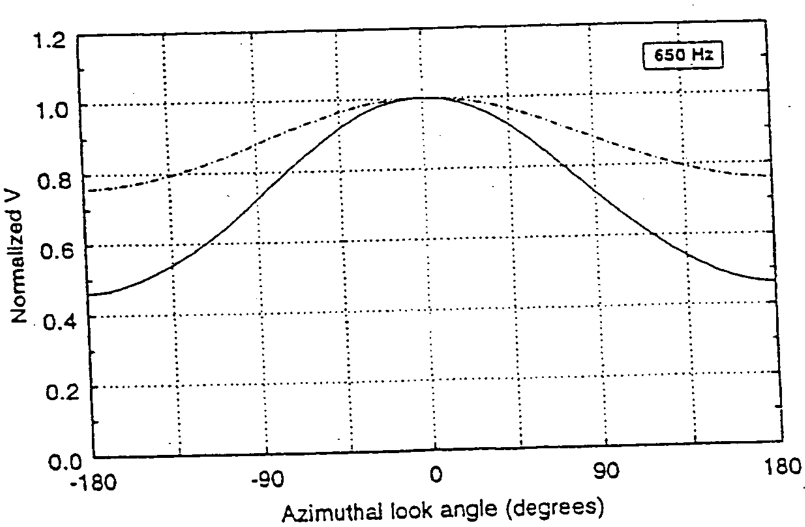

FIG 6

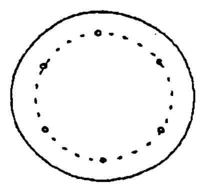

FIG 10A

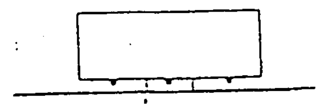

FIG 10B

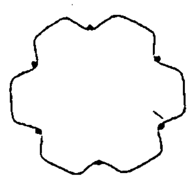

FIG 11A

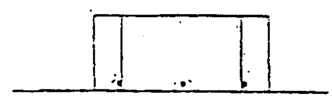

FIG 11B

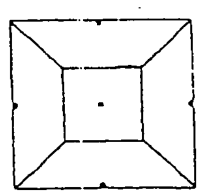

FIG 12A

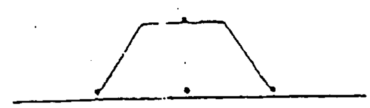

FIG 12B

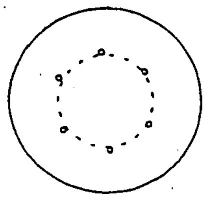

FIG 16A

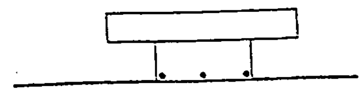

FIG 16B

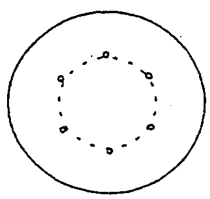

FIG 17A

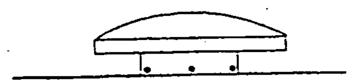

FIG 17B

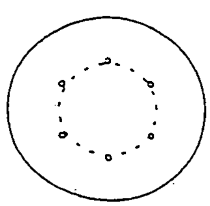

FIG 18A

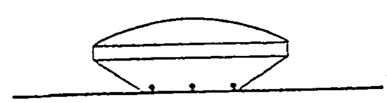

FIG 18B

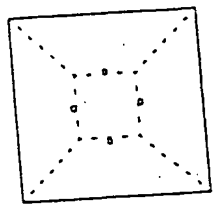

FIG 22A

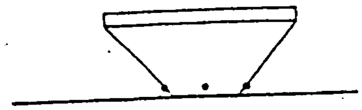

FIG 22B

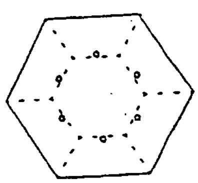

FIG 23A

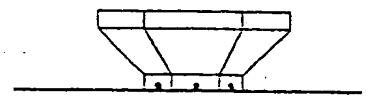

FIG 23B

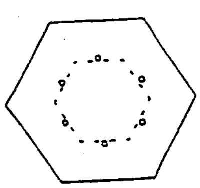

FIG 24A

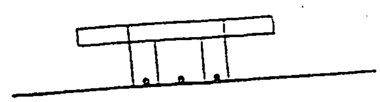

FIG 24B

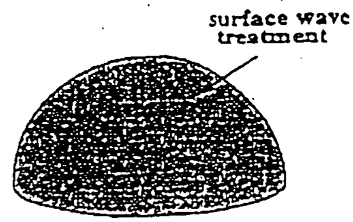

FIG 28

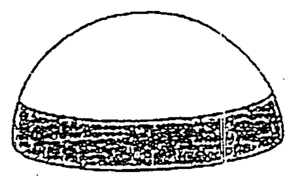

FIG 29

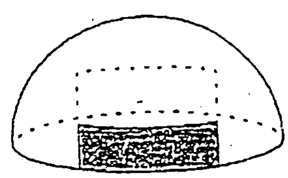

FIG 30

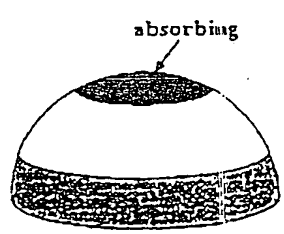

FIG 31

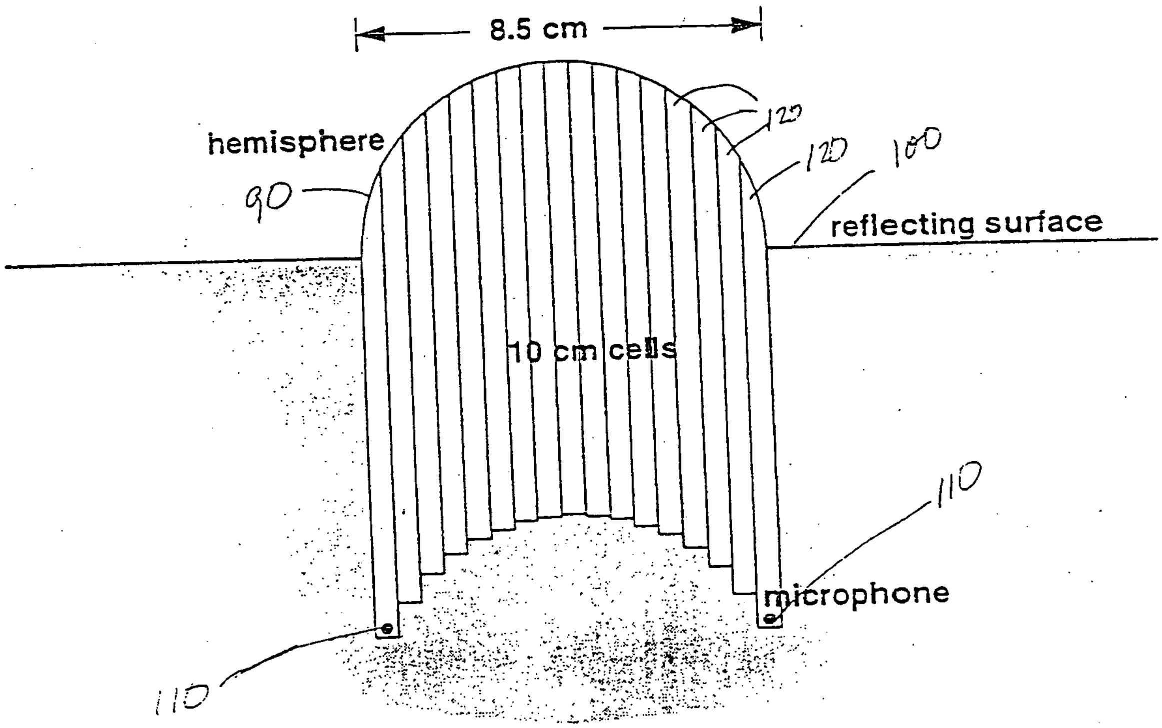
8.5 cm
hemisphere
90
120
120
100
reflecting surface
10 cm cells
110
microphone
110

FIG 34